Surface alloying of titanium with nickel by using cathodic arc based plasma treatment

Nagihan Sezgin[*1], Erkan Kaçar[2], Kürşat Kazmanlı[3], Mustafa Ürgen[4]

ABSTRACT

In this study, cathodic arc electron / metal ion treatment (CA-EMIT) technique was used to modify Ti surfaces in Ni cathodic arc plasma. At this novel method, AC bias was applied to the Ti substrates. In positive cycle of AC bias, the substrates were heated by electrons while nickel ions were directed toward the substrate surface in negative cycle. The surface modification processes were performed at 5 different temperatures: 1073 K (800 °C), 1273 K (1000 °C), 1373 K (1100 °C), 1473 K (1200 °C) and 1573 (1300 °C). The samples were characterized by XRD, SEM and EDS analysis. The effect of substrate temperature and cathode current were investigated on microstructure of the samples. This process provides rapid diffusion of nickel into the titanium and high diffusion depths were obtained compared to literature studies.

Keywords: Ni-Ti, diffusion, intermetallics, cathodic arc pvd, plasma treatment

1. INTRODUCTION

Diffusion in the binary Ni-Ti system has been the subject of a substantial number of studies aiming mainly to investigate the diffusion behavior between these two metals for powder metallurgy and brazing applications [1-10]. The major goal in these studies was to obtain and understand the mechanism of formation of the well-known NiTi phase by solid-state diffusion processes. This phase is of considerable technological interest due to its superelasticity, shape memory and excellent tribological properties [11-12]. Additionally, $NiTi_2$ intermetallic and its composites is another group of materials of interest since this phase is the hardest phase in Ni-Ti system [13].

In the Ti rich side of Ti-Ni binary system [14], low temperature stable hexagonal α-Ti, which has a very low solubility of Ni, and high temperature stable cubic β-Ti with a high solubility of nickel are present. By the increase of nickel content, the Ni-Ti phases in the binary phase appear as stable compounds in the order of $NiTi_2$, NiTi, Ni_3Ti intermetallics and Ni-Ti solid solutions. Phase formations in Ni-Ti system was investigated depending on many parameters such as process temperature, time, surface roughness, and grain size of powder in different diffusion based studies.

Bastin and Rieck [1, 2] performed extensive experiments in Ni-Ti system including different diffusion couples in the binary phase diagram and determined the formation mechanism of the phases and the intrinsic diffusion coefficients.

$NiTi_2$ and Ni_3Ti formed earlier than NiTi when the diffusion couple is elemental Ni and Ti. Also Laeng et al [4] studied the phase formations via solid state reaction of Ni-Ti powder mixtures. They reported that NiTi could not be formed via interdiffusion of elemental Ni and Ti that is determined by lower Gibbs free energy of formation when compared to $NiTi_2$ and Ni_3Ti same as Bastin and Rieck. NiTi formation is possible only by the reaction of Ni_3Ti and $NiTi_2$ phases. But reaction is very slow and NiTi formation has difficulties with increasing diffusion lengths and barriers. Shao et al [5,6] explained the same results from the different point of interface energies. At these studies, the last formed phase was determined as NiTi, but the first formed phase was not exactly known.

Beside these studies, some resarchers studied the effect of the external current of heating rate on the phase formations [3, 7, 8]. Application of external current to the samples increased the diffusion rate at the study of Garay et al. A coating/diffusion process of Ni-Ti system was studied by Rampin et al. [10]. They investigated the heat treatment temperature effect on the diffusion of Ni, resulting microstructure and hardness of titanium substrate.

Although there are number of diffusion studies for Ni-Ti system in literature, the researcher still did not come to an agreement on the NiTi formation mechanism and the intermetallic formation sequence. However, difficulty of the NiTi formation due to Gibbs free energy and nucleation energy is the common results reported in literature. In these studies, because the diffusion couple is in solid phase, the diffusion rate depended on the intermetallic formed at the interface and the contact barriers between the couple. If the one of the couple is in vapor phase, the contact barriers can be low enough to increase the diffusion rate.

In this study, we aimed to alloy titanium substrates with the Cathodic Arc PVD deposited nickel benefiting from the unique properties of cathodic arc process. One of them is the ability of producing highly ionized plasma containing sufficient amount of ions and electrons. In conventional CA-PVD processes the substrate is negatively biased to increase the density and integrity of the coating by accelerating the ions towards the substrate and the electrons are directed to the ground, which is the walls of deposition chamber [17, 18]. These electrons can be used for heating the substrate through Joule

heating effect if they can be directed towards the substrate instead of the walls of the vacuum chamber [19]. We have benefited from these electrons for heating the substrate by negatively biasing the substrate. The process will be named hereafter as cathodic arc electron / metal ion treatment (CA-EMIT) [15, 16]. This process has been first utilized in our group for studying of aluminizing of Ni and Ti [15, 20].

In CA-EMIT technique, maximum bias voltage of 30 V AC (50 Hz) was used to utilize both deposition (in negative cycle) and electron heating process (in positive cycle) sequentially. In the negative cycle of AC bias, the ions were accelerated and deposited on the sample. In following positive cycle, flow of electrons in the plasma through the sample results in Joule heating of the surface (Fig. 1). Using electrons for heating effectively increased the substrate temperature and allowed the diffusion between the deposited metal and the substrate.
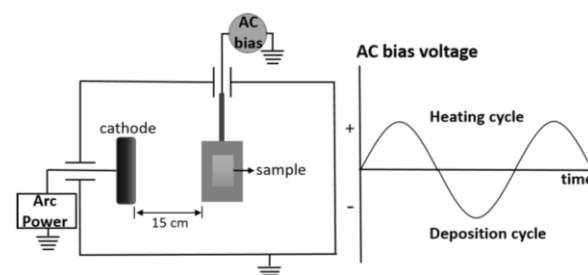

Figure 1. Schematic view of the CA-EMIT method.

By the utilization of this method it becomes possible to tune both the amount of deposited material and substrate temperature by increasing or decreasing the cathode current and magnitude of AC bias respectively. The lack of surface contact barrier is another advantage of the method. The deposited metal is in direct contact with the substrate that is free from its oxides, since the process is conducted in vacuum and the deposited metal covers the entire surface independent of its surface roughness. These differences when compared to conventional methods in which the elements of the couple were put together and then diffusion was ensured by heat treatment are expected to exert substantial effects on the kinetics of diffusion and on the formed phases and microstructures. At this study, the main aim is investigating the diffusion mechanism of Ni-Ti couple and formation sequence of phases in this new method (CA-EMIT). On the other hand, alloying of titanium substrates could be achieved in one process, without a post heat treatment.

2. EXPERIMENTAL

Pure Ti (99.5%) plates with 20x30 mm dimension and 1 mm thickness were polished by using up to 1200 grid grinding paper and then ultrasonically cleaned in ethanol and acetone for 10 minutes. Shortly after polishing, the samples were placed in the vacuum chamber and ion-treated in nickel + argon plasma. Nickel cathode diameter was 10 cm and the distance between cathode and the substrate was 15 cm. Before CA-EMIT procedure, the vacuum chamber was evacuated down to approximately 5×10^{-3} Pa base pressure. The plasma was created by cathodic arc evaporation of nickel at 1×10^{-1} Pa argon pressure. Nickel cathode current was 90 A. AC bias voltage (f: 50 Hz) was applied to the samples to heat the substrates to temperatures above the eutectoid point (1038 K (765 °C)), which were 1073 K (800 °C), 1273 K (1000 °C), 1373 K (1100 °C), 1473 K (1200 °C) and 1573 K (1300 °C). Additionally, in order to investigate the plasma ion flux effect on the structure, the cathode current was increased to 110 A for 1373 K (1100 °C) treatment temperature.

Table 1. CA-EMIT process parameters.

Sample	AC Bias		Subs Temp., ±20
	V	A/cm^2	
1	7	0.26	1073 K (800 °C)
2	13	0.35	1273 K (1000 °C)
3	14	0.40	1373 K (1100 °C)
4	15	0.46	1473 K (1200 °C)
5	16	0.51	1573 K (1300 °C)

The CA-EMIT process parameters are listed in Table 1. The substrate temperature was monitored and recorded by using an infrared pyrometer (Dias Pyrospot DG 10N). Total ion treatment time was 30 minutes for each sample.

After electron-metal ion treatment, the phase constituents on the sample surfaces were identified by x-ray diffraction (XRD) technique. XRD analyses were carried out over the 2θ range (symmetric geometry scan mode) of 20-90° by Philips PW 3710 diffractometer with Cu Kα radiation source, generated by 40 kV and 40 mA. Cross section morphologies of the samples were investigated by scanning electron microscope and the morphology observed in the cross-section micrographs were correlated with the XRD results. The nickel/titanium ratios of each phase in

the SEM cross-section micrograph were measured using Oxford Instruments-7557, energy dispersive x-ray spectroscopy (EDS).

3. RESULTS AND DISCUSSION

3.1 Titanium samples treated at 1073 K (800 °C) and 1273 K (1000 °C)

The results of structural and phase investigations of the Ni cathodic arc plasma treated Ti at 1073 K (800 °C) and 1273 K (1000 °C) treatment temperatures are given below. In the diffraction pattern of the titanium substrate, which was treated at 1073 K (800 °C), by cathodic arc nickel plasma, the main discernible phase was nickel (Fig. 2). Along with the nickel peaks, there were also small peaks of α-Ti, Ni_3Ti, $NiTi_2$ and $NiTi$ intermetallic phases.
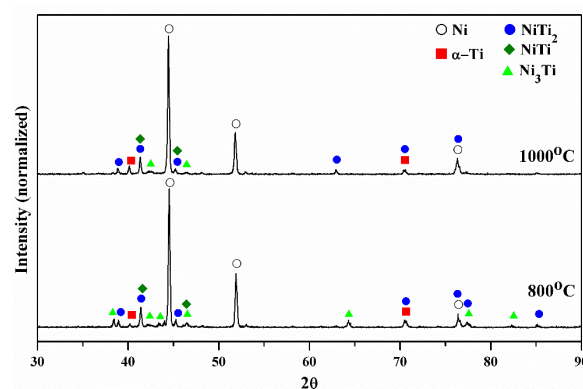

Figure 2. The XRD diagrams of the samples treated at 1073 K (800 °C) and 1273 K (1000 °C)

The SEM cross-section micrograph of the same sample, exhibited a layered surface structure (Fig. 3). The EDS analysis results indicated that these layers were $NiTi_2$ (region IV), Ni_3Ti (region II) intermetallics and Ni deposit (region I). Additionally, it was determined that $NiTi$ phase (marked with III in the Fig. 3) was dispersed in the $NiTi_2$ layer. Below these intermetallic layers, nickel diffused into Ti substrate and a eutectoid $(\alpha+NiTi_2)$ structure was formed in some regions below intermetallic layers. There was not a distinct homogenous Ni diffusion layer.
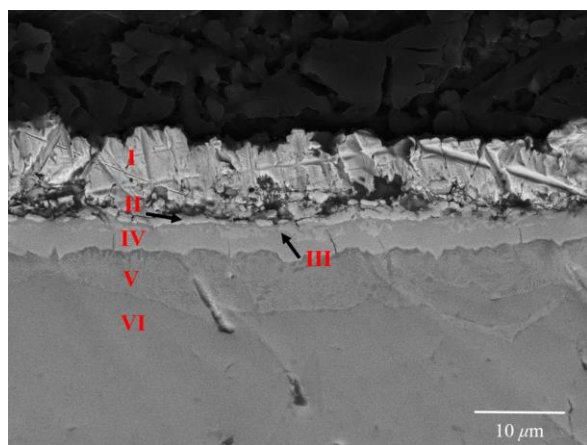
Figure 3. Backscattered SEM micrograph of the cross section of the sample treated at 1073 K (800 °C); I: Ni deposit, II: Ni$_3$Ti layer, III: NiTi precipitates, IV: NiTi$_2$ layer, V: Ni containing Ti region (eutectoid zone), VI: Ti substrate
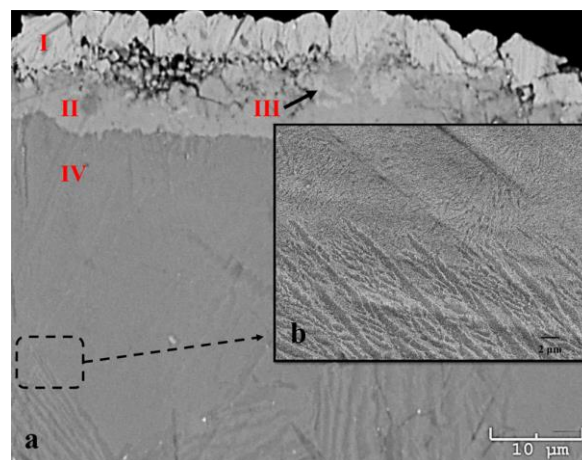

Fig. 4. Backscattered SEM micrograph of sample treated at 1273 K (1000 °C), a: I: Ni deposit, II: NiTi$_2$ layer, III: NiTi precipitates IV: Ti (Ni), b: high magnification of the dashed rectangle area that is the interlayer of two different regions.

According to the Ni-Ti binary phase diagram [14], the sequence of intermetallics followed by the metallic nickel layer should be in the order of Ni$_3$Ti, NiTi and NiTi$_2$. However, the results of SEM investigations for the sample treated at 1073 K (800 °C) NiTi has not been observed as a separate layer. In literature [1, 4, 5, 21], it was reported that Ni$_3$Ti and NiTi$_2$ intermetallics could form before NiTi due to their lower Gibbs free (formation) energies than that of NiTi. Besides, interface energies of Ni$_3$Ti and NiTi$_2$ intermetallics are lower than NiTi therefore they might nucleate before NiTi phase. According to the literature [4], formation of NiTi via solid state diffusion process is also kinetically slower than the other intermetallics in Ni-Ti system. Thus the NiTi phase observed within NiTi$_2$ layer close to Ni$_3$Ti interface could have formed in consequence of interactions between these two intermetallics.

When the treatment temperature was increased to 1273 K (1000 °C), the diffusion rate of nickel into the titanium substrate increased. The XRD pattern of the sample treated at 1273 K (1000 °C) was given at Fig. 2. The XRD patterns and SEM cross sections of the samples treated at 1073 K (800 °C) and 1273 K (1000 °C) exhibited similar features. Along with the main nickel peaks, there were also α-Ti, NiTi$_2$, NiTi and Ni$_3$Ti phase peaks similar to the ones for the sample treated at 1073 K (800 °C). However, the intensity of the Ni$_3$Ti peaks became lower with the increase of the temperature.

Similar layered structure of nickel deposit (Fig. 4a, region I) and NiTi$_2$ phase (Fig. 4a, region II) with NiTi precipitates (Fig. 4a, region III) was obtained at 1273 K (1000 °C). Thickness of the nickel deposit layer reduced compared to 1073 K (800 °C) sample as seen in Fig. 4a. On the other hand, the NiTi$_2$ intermetallic layer below the nickel deposit became thicker. Similar to the 1073 K (800 °C) sample, NiTi intermetallic phase was dispersed in the NiTi$_2$ layer. Although small intensity Ni$_3$Ti diffraction peaks existed in the XRD pattern, Ni$_3$Ti phase was not observed in the SEM micrographs. This phase may exist as small sized dispersoids in the nickel deposit or a very thin layer at the interface between NiTi$_2$ and Ni.

Major structural difference between the samples that were treated at 1073 K (800 °C) and 1273 K (1000 °C) is the presence of a 100 µm thick nickel containing zone (Fig. 4a and b) below the intermetallics at 1273 K (1000 °C). This observation indicated that before formation of the intermetallic layers, substantial amount of nickel diffusion took place. This is an expected result since the treatment is conducted at a temperature where β titanium (solid solution region between Ni and Ti) is stable in which diffusion of nickel into titanium is very fast because of the change in the lattice of Ti from hcp to bcc. Diffusion of nickel is then limited after the enrichment of nickel on the surface to a concentration that is sufficient for the formation of the NiTi$_2$ intermetallic. The diffusion zone below the intermetallic consisted of two layers with distinct morphological differences. The layer adjacent to the NiTi$_2$ intermetallic (region IV at Fig 4a and upper side of Fig 4b) has a fine eutectoid (α+

NiTi$_2$) structure with a thickness of approximately 30 μm. The nickel content of this layer at the interface was 8.17 at.% and decreased gradually to 6.18 at.% at the end of the fine eutectoid structure. When the nickel concentration decreased, a coarse lamellar structure (Widmanstatten) became apparent (lower side of Fig 4b). The difference in nickel content of these layers might be the reason of the morphological change. According to Rampin [10] Widmanstatten structure formation is diffusion-controlled process and can form at low nickel concentrations. During the formation of this structure, α phase is nucleated at the β grain boundaries.

3.2 Titanium samples treated at 1373 K (1100 °C), 1473 K (1200 °C) and 1573 K (1300 °C)

When the treatment temperature was increased above 1273 K (1000 °C), significant changes took place in the structure and phase. The diffraction patterns of the samples that were treated at 1373 K (1100 °C), 1473 K (1200 °C) and 1573 K (1300 °C), were composed of α-Ti and eutectoid α + NiTi$_2$ phases (Fig. 5). From the XRD patterns it can be seen that, with increasing temperature, the intensity of NiTi$_2$ phase peaks decreased indicating a decrease of nickel content in the layer.
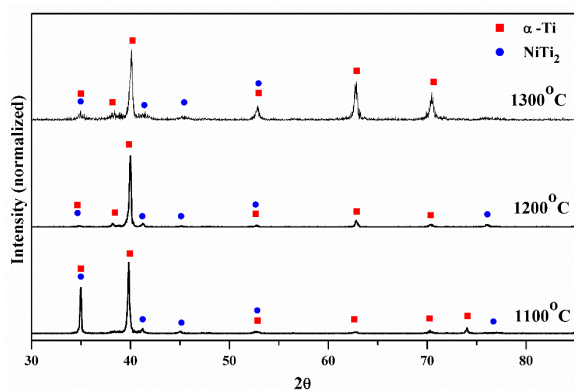
Fig. 5. The XRD diagrams of the samples treated at 1373 K (1100 °C), 1473 K (1200 °C) and 1573 K (1300 °C)

At 1373 K (1100 °C), 1473 K (1200 °C) and 1573 K (1300 °C) treatment temperatures, there was also notable differences in the cross sectional morphology compared to 1073 K (800 °C) and 1273 K (1000 °C) treated samples. On the cross section SEM images of these samples (Fig. 6a, b and c) nickel deposit and intermetallic layers were not observed, indicating a high rate of diffusion of Ni into Ti. In the cross sections of these samples a lamellar structure that formed as a result of eutectoid reaction at 1038 K (765 °C) is evident.
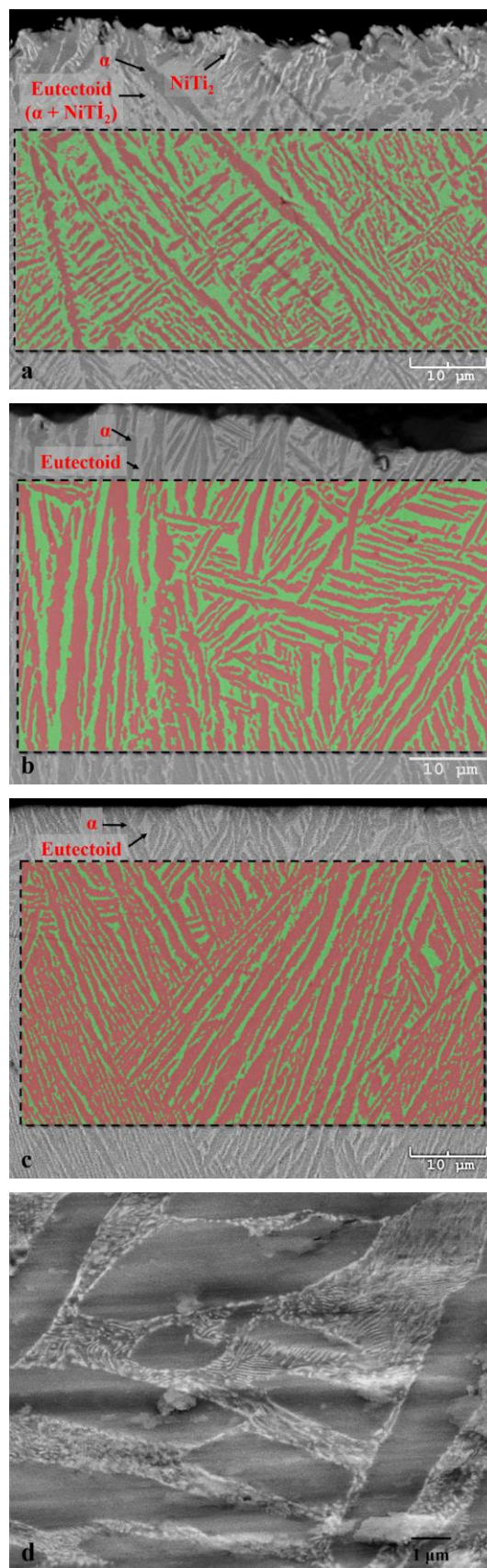
Fig. 6. Backscattered SEM micrographs of samples treated at a) 1373 K (1100 °C), b) 1473 K (1200 °C), c) 1573 K (1300 °C). From the dashed rectangles α/eutectoid ratios were calculated, d) higher magnification of eutectoid (α + NiTi$_2$) region.

Dark areas in the backscattered electron micrograph corresponds to α-Ti. Brighter regions consist of eutectoid structure composed of fine α-

Ti and NiTi$_2$ platelets (Fig 6d). In literature [6, 22], there are studies that define such lamellar microstructures for Ni-Ti system, as α+β structure that needs further verification by higher magnification images of the "so called β regions" and physical metallurgy principles. The lamellar structures were getting coarser and longer with increasing temperature thereof the decreasing Ni content. The nickel concentrations in the regions close to the surface were 11 at. %, 8 at. % and 7 at. % for 1373 K (1100 °C), 1473 K (1200 °C) and 1573 K (1300 °C) samples, respectively. According to the binary phase diagram of Ni-Ti, these nickel concentrations correspond to solid β + liquid phase regions at these treatment temperatures. Faster diffusion of nickel at higher temperature kept the nickel concentrations lower so that the sample surfaces comprised very thin β + liquid zone. However, there was not any discernable structural change related with this β + liquid zone observed in SEM micrographs (Fig 6a, b and c). Below this thin solid+liquid phase zone, there were β-Ti region that diffusion took place in solid state at the temperatures higher than 1273 K (1000 °C). The nickel amount of these solid regions were lower than 7.7 at%, 5.8 at% and 4.2 at% for 1373 K (1100 °C), 1473 K (1200 °C) and 1573 K (1300 °C), respectively. Among these high temperature samples only 1373 K (1100 °C) sample had NiTi$_2$ intermetallic phase precipitates observed in the SEM micrographs close to surface (white regions in Fig. 6a).
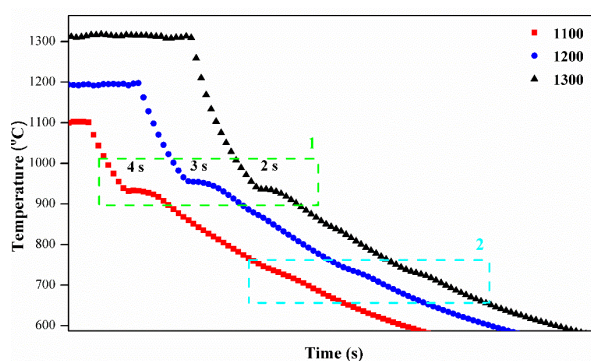

Fig. 7. Cooling curves of the samples treated at 1373 K (1100 °C), 1473 K (1200 °C) and 1573 K (1300 °C)

A quantitative image analysis was carried out on the SEM images (the dashed rectangle area in Fig. 6a, b and c). "Materials Image Processing and Automated Reconstruction" (MIPAR) software was used to calculate α – eutectoid (α + NiTi$_2$) ratio [23]. The amount of α (darker sides in Fig. 6a, b and c) and eutectoid (lighter sides in Fig. 6a, b and c) in the diffusion zone changed depending on the treatment temperatures. The alpha ratio

increased from 49% to 60% and 74% as the temperature increased from 1373 K (1100 °C), 1473 K (1200 °C) and 1573 K (1300 °C), respectively. By increasing temperature, the nickel concentrations decreased as a result of higher Ni diffusion rate and therefore, the ratio of α-Ti increased.

During the CA-EMIT process, substrate temperature was monitored by an infrared pyrometer and from this data 'temperature-cooling time' diagrams (Fig. 7) were drawn. The 'Temperature – Cooling Time' diagrams had plateaus at about 1223 K (950 °C) for samples treated at 1373 K (1100 °C), 1473 K (1200 °C) and 1573 K (1300 °C). In titanium rich side of Ni-Ti binary phase diagram [14], eutectic phase transformation takes place at about 1220 K (947 °C). The observed plateaus (dashed rectangle 1) in the cooling curves were close to the eutectic transformation temperature. The cooling rates were 2200 K/min for 1573 K (1300 °C) 1300 °C sample, 1450 K/min for 1473 K (1200 °C) sample and 1380 K/min for 1373 K (1100 °C) sample. While cooling the samples, the liquid + β phases transformed to β + NiTi$_2$. The transformation times were slightly longer for the samples treated at lower temperatures and took 4, 3 and 2 seconds for samples treated at 1373 K (1100 °C), 1473 K (1200 °C) and 1573 K (1300 °C), respectively. The transformation time in eutectic temperature is related to the amount of liquid to be solidified and the shortest time was for the 1573 K (1300 °C) sample for which the amount of liquid phase is minimum. Since the diffusion was faster at higher temperatures, nickel concentration became lower along the diffusion zone (refer to binary phase diagram). Therefore, at higher temperature, amount of the liquid phase on the sample surface was lower and diffusion proceeded faster.

During cooling the samples to the room temperature transformation of the β phase to α + NiTi$_2$ phases occur at the eutectoid temperature (1038 K (765 °C)). Because eutectoid transformation takes place in the solid-state, distinctive eutectoid isotherms were not clearly observed in the cooling curves (dashed rectangle 2 in Fig. 7). There was only a slight change in slope of the cooling curves (Fig. 7) around eutectoid transformation temperature.
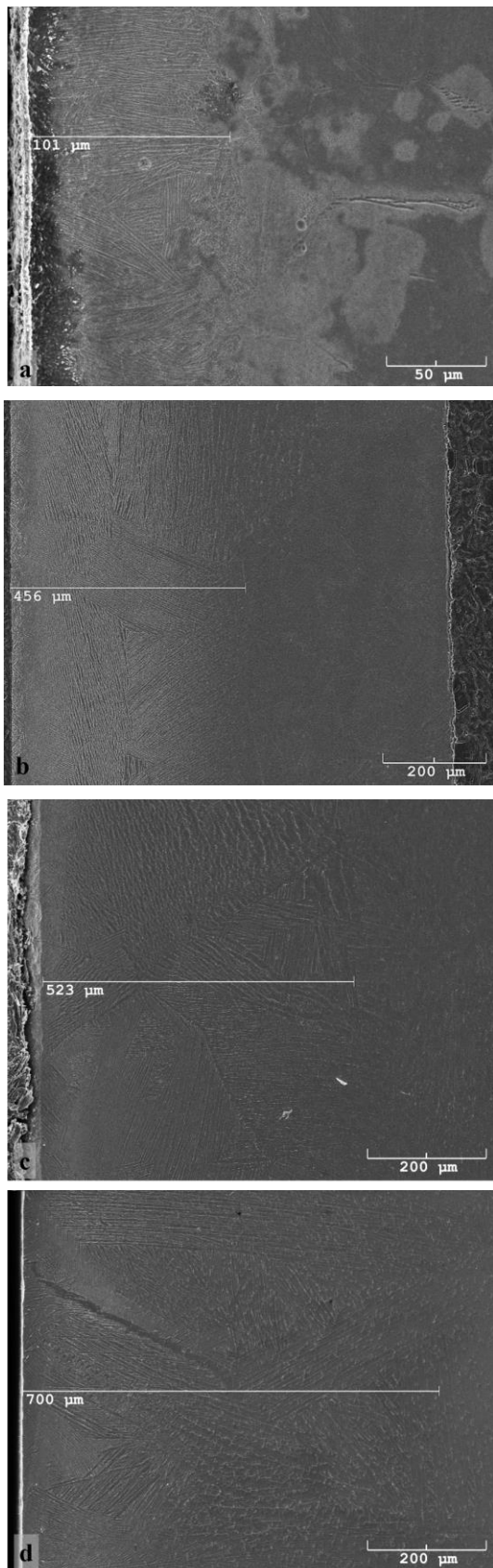
Figure 8. SEM images of the etched samples that give the diffusion depths, treated at a) 1273 K (1000 °C), b) 1373 K (1100 °C), c) 1473 K (1200 °C), d) 1573 K (1300 °C).

The measured diffusion depths for 1373 K (1100 °C), 1473 K (1200 °C) and 1573 K (1300 °C) samples were 101 µm, 456 µm, 523 µm and 700 µm, respectively (Fig 8). The nickel diffusion depth of the sample 1273 K (1000 °C) was considerably low comparing the other samples treated at 1373 K (1100 °C), 1473 K (1200 °C) and 1573 K (1300 °C). The intermetallic layers formed on 1273 K (1000 °C) sample obviously limited the nickel diffusion. Intermetallic phase formation is related to nickel flux in the plasma and diffusive mass flux of nickel in the substrate. When diffusive mass flux of nickel is lower than plasma nickel flux, nickel deposits and intermetallic Ni-Ti layers formed on the surface. The diffusion rate of the nickel increased at the temperatures above 1273 K (1000 °C), the intermetallic layers limiting the nickel diffusion was not formed and nickel could diffuse to longer distances.
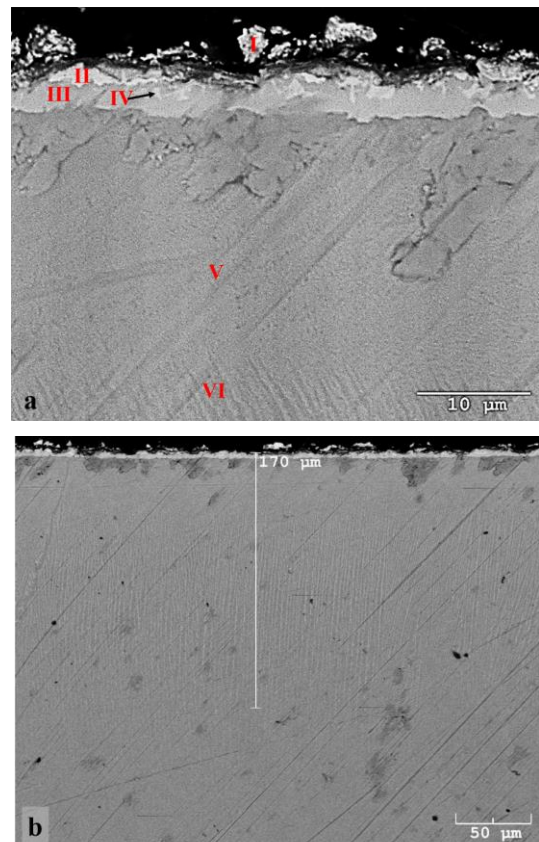

Figure 9. Backscattered SEM micrographs of samples treated at 1373 K (1100 °C), 110A cathode current, a) I: Ni deposit, II: Ni3Ti layer, III: NiTi2 layer, IV: NiTi precipitates, b) diffusion depth.

In order to investigate the effect of nickel ion flux on formation of phases and diffusion an additional experiment was carried out at 1373 K (1100 °C) for 30 minutes by using higher nickel ion flux. Nickel cathode current, which is directly related with ion flux, was increased to 110 A. The temperature was adjusted by changing the AC voltage so as to keep the temperature at 1373 K (1100 °C). The SEM micrographs of the sample were given in Fig 9. When the nickel ion flux increased, a deposit layer, which composed of

nickel and intermetallic phases, was formed on the sample. The phases in the deposit layer (Fig. 9a) were nickel (I), Ni$_3$Ti (II), NiTi$_2$ (III), NiTi (IV). Similar to 1273 K (1000 °C) sample, there were two different regions showing fine structured (region V) and lamellar morphologies (region VI) within the diffusion zone below the deposit layer. Obviously, the deposit layer affected the morphology of the diffusion zone and promoted the formation of a fine structured morphology as seen in Fig. 9. Besides, the diffusion depth of the nickel decreased to 170 μm as shown in Fig. 9b. The decrease in diffusion depth also shows the limiting effect of the intermetallic layers.

4. CONCLUSIONS

In the present study, Ti surfaces were modified by Ni plasma using CA-EMIT method. Layered structures formed on the samples treated at 1073 K (800 °C) and 1273 K (1000 °C). The top layer was nickel deposit and beneath this layer there were intermetallic layers, which were consisted of Ni$_3$Ti and NiTi$_2$ respectively. NiTi intermetallic phases dispersed at the interface between the Ni$_3$Ti and NiTi$_2$ layers. Although promoter intermetallics form as layers during the treatment, it was not possible to obtain separate layers of NiTi, highly probably related to the sluggishness of the NiTi formation reaction.

For the sample treated at 1273 K (1000 °C), 100 μm diffusion zone was formed, which indicated a fast diffusion zone formation until the nickel concentration reaches to a value sufficient for intermetallic formation. The layered structure was not observed at temperatures higher than 1273 K (1000 °C). The measured nickel diffusion depths for 1373 K (1100 °C), 1473 K (1200 °C) and 1573 K (1300 °C) samples were 456 μm, 523 μm and 700 μm, respectively. The diffusion zone of these samples were consisted of α-Ti + eutectoid lamellar structure. When the treatment temperature increased, concentration of α-Ti increased as well. The diffusion layer thicknesses are almost two times higher when compared to studies conducted using Ni-Ti bulk material couples [10] which can be attributed to elimination of diffusion barriers and flow of current through the substrate during the treatment [3].

The diffusion rate and the nickel ion flux had a critical effect on the layer formation and diffusion zone. In the experiments conducted at 1373 K (1100 °C) for two different nickel vapor flux, for cases where the diffusion rate of nickel is lower than nickel vapor flux, nickel deposits and intermetallic Ni-Ti layers formed on the surface (Fig. 9). On the other hand, .in the case of lower nickel vapor flux, because of high rate of nickel diffusion, nickel amount could not reach to the concentrations sufficient for intermetallic layers formation (Fig. 6a).

CA-EMIT is a promising technique for diffusion alloying of metal surfaces and for studies on diffusion kinetics with its ability to tune both temperature and metal flux during processing.

REFERENCES

[1] G. F. Bastin and G. D. Rieck, Diffusion in the Titanium-Nickel System: I. Occurrence and Growth of the Various Intermetallic Compounds, Metall. Trans., 1974, vol. 5, pp. 1817-26.

[2] G. F. Bastin and G. D. Rieck, Diffusion in the Titanium-Nickel System: II. Calculations of Chemical and Intrinsic Diffusion Coefficients, Metall.Trans, 1974, vol. 5, pp. 1827-31.

[3] J.E. Garay, U. Anselmi-Tamburini 1, Z.A. Munir, Enhanced growth of intermetallic phases in the Ni–Ti system by current effects, Acta Mater., 2003, vol. 51, pp. 4487-95.

[4] J. Laeng, Z. Xiu, X. Xu, X. Sun, H. Ru and Y. Liu, Phase formation of Ni–Ti via solid state reaction, Phys. Scr., 2007, vol. T129, pp. 250–254.

[5] X. Shao, X. Guo, Y. Han, Z. Lin, J. Qin, W. Lu and D. Zhang, Preparation of TiNi films by diffusion technology and the study of the formation sequence of the intermetallics in Ti–Ni systems, J. Mater. Res., 2014, vol. 29, pp. 2707-16.

[6] X. Shao, X. Guo, Y. Han, W. Lu, J. Qin, D. Zhang, Characterization of the diffusion

bonding behavior of pure Ti and Ni with different surface roughness during hot pressing, Mater. Des., 2015, vol. 65, pp. 1001–10.

[7]   P. Novák, L. Mejzlíková, A. Michalcová, J. Capek, P. Beran, D. Vojtech, Effect of SHS conditions on microstructure of NiTi shape memory alloy, Intermetallics, 2013, vol. 42, pp. 85-91.

[8]   P. Novák, P.Pokorný, V. Vojtech, A. Knaislova, A. Skolakova, J. Capek, M. Karlík, J. Kopecek, Formation of Ni-Ti intermetallics during reactive sintering at 500-650 °C, Mater. Chem. Phys., 2015, vol. 155, pp. 113-121.

[9]   A. Elrefaey, L. Wojarski, J. Janzcak-Rusch and W. Tillmann, Vacuum brazing titanium using thin nickel layer deposited by PVD technique, Mater. Sci. Eng. A, 2013, vol. 565, pp. 180-186.

[10]   I. Rampin, K. Brunelli, M. Dabalà, M. Magrini, Effect of diffusion of Ni and B on the microstructure and hardness of Ti Cp, J. Alloys Compd., 2009, vol. 48, pp. 1246–53.

[11]   D.Y. Li, A new type of wear-resistant material: pseudo-elastic TiNi alloy, Wear, 1998, vol. 22, pp. 1116–23.

[12]   H.Hiraga, T. Inoue, H. Shimura, A. Matsunawa, Cavitation erosion mechanism of NiTi coatings made by laser plasma hybrid spraying, Wear, 1999, vol. 231, pp. 272-278.

[13]   F. Gao and H.M. Wang, Dry sliding wear property of a laser melting/deposited Ti_2Ni/TiNi intermetallic alloy, Intermetallics, 2008, vol. 16, pp. 202-208.

[14]   Murray J. L., ASM Handbook vol. 3: Alloy Phase Diagrams, ASM International, USA, 1992, pp. 319.

[15]   S. Oncel, Production of NiAl thermal barrier bond coats by cathodic arc aluminium plasma treatment, Doctoral Dissertation, Istanbul Technical University, Institute of Science and Technology, Turkey, 2012.

[16]   S. Oncel and M. Urgen, Method for controlled production of diffusion based coatings by vacuum cathodic arc systems, Patent, EP 2829635 A1, Jan 28, 2015.

[17]   J. L. Vossen and W. Kern, Thin Film Processes II, Gulf Publishing, San Diego-CA, 1991, pp. 210-218.

[18]   S. M. Rossnagel, J. J. Cuomo, W. D. Westwood, Handbook of plasma processing technology, Noyes Publication, New Jersey, 1990, pp. 419-430.

[19]   J. Vetter and A. J. Perry, Advances in cathodic arc technology using electrons extracted from the vacuum arc, Surf. Coat. Technol., 1993, vol. 61, pp. 305-309.

[20]   T. Turutoglu, Alloying of titanium surfaces by cathodic arc aluminum plasma, Doctoral Dissertation, Istanbul Technical University, Institute of Science and Technology, Turkey, 2013.

[21]   V.I. Nizhenko, Free surface energy as a criterion for the sequence of intermetallic layer formation in reaction couples, Powder Metall. Met. Ceram., 2004, vol. 43, pp. 273-279.

[22]   S. Kundu and S. Chatterjee, Characterization of diffusion bonded joint between titanium and 304 stainless steel using a Ni interlayer, Mater. Charact., 2008, vol. 59, pp. 631-637.

[23]   J.M. Sosa, D.E. Huber, B. Welk, H.L. Fraser, Development and application of MIPAR^{TM}: a novel software package for two- and three-dimensional microstructural characterization, Integr. Mater. Manuf. Innov., 2014, vol.3, pp. 18